Three-Dimensional FEM Rotordynamics and the So-Called Centrifugal Softening of Rotors

Acc. Sc. Torino
Memorie Sc. Fis. 36 (2012) MECCANICA DEI SOLIDI

Three-Dimensional FEM Rotordynamics and the So-Called Centrifugal Softening of Rotors

Memoria di GIANCARLO GENTA e di MARIO SILVAGNI[*]
presentata dal Socio nazionale Giancarlo GENTA nell'adunanza del 14 dicembre 2011
e approvata nell'adunanza dell'8 febbraio 2012

Abstract. *Centrifugal softening effect is an alleged and elusive reduction of the natural frequencies of a rotating system with increasing speed sometimes found in finite element rotordynamics. This reduction may, in some instances, be large enough to cause some of the natural frequencies to vanish, leading to a sort of elastic instability. Some doubts can be however cast on the phenomenon in itself and on the mathematical models causing it to appear. The aim of the present work is to shed some light on centrifugal softening and to discuss the assumptions that are at the basis of 3-dimensional finite element (FEM) modeling in rotordynamics.*

Keywords: rotordynamics, FEM, natural frequencies, centrifugal stiffening.

Riassunto. *L'effetto che viene spesso definito 'centrifugal softening' consiste in una riduzione delle frequenze proprie di un sistema rotante all'aumentare della velocità, che viene talvolta osservato nello studio dinamico dei rotori quando si usa il metodo degli elementi finiti. In alcuni casi questa diminuzione è tanto pronunciata da portare a zero alcune frequenze proprie, causando una sorta di instabilità elastica. Si possono tuttavia formulare seri dubbi sul fenomeno in sé e sui metodi di calcolo che lo evidenziano. Scopo del presente lavoro è di chiarire il fenomeno e di discutere le ipotesi che stanno alla base della modellazione tridimensionale mediante il metodo degli elementi finiti (FEM) nella dinamica dei rotori.*

Parole chiave: dinamica dei rotori, metodo degli elementi finiti.

1. Introduction

In spite of the fact that rotordynamics has a long tradition and that most of the issues linked with the dynamic behaviour of rotating machines seemed to be well understood since a long time, some points are still liable to produce misunderstandings. Problems may occur even when trying to solve problems as basic as computing the Campbell diagram and the critical speeds of linear, axi-symmetric rotors running on axi-symmetric bearings and stator, when one tries to go beyond the classical and well understood beam-like modelling.

[*] Mechatronics Lab., Politecnico di Torino, Italy.

The classical approach to rotordynamics is based on the so-called 1-dimensional (1-D) model, in which the shafts are modelled as beams and discs and other parts of the rotor that extend in the radial direction are modelled as rigid bodies. In time a number of models based on this approach were developed, from the simplest Jeffcott rotor (2 d.o.f.), to the slightly more complex rotor with 4 d.o.f., to models based on the lumped parameter approach, on the transfer matrices method and finally on the Finite Element Method (FEM) [1, 2, 3]. In all cases, there is a complete uncoupling between axial, torsional and bending behaviour of rotors, and usually rotordynamics deals only with the latter.

If the rotor is axially symmetrical, its free dynamic behaviour is studied in an inertial reference frame, and the relevant linearized homogeneous equation of motion (for the undamped system) has the following structure [3]:

$$\mathbf{M}\ddot{\mathbf{q}} + \Omega\mathbf{G}\dot{\mathbf{q}} + \mathbf{K}\mathbf{q} = 0 \quad . \tag{1}$$

where **M** and **K** are the usual mass and stiffness matrix and **G** is the gyroscopic matrix. The first is always symmetric, the second is usually such while the third is skew symmetric.

As an alternative, the equation of motion can be written using the complex coordinates approach, and the gyroscopic term is imaginary while the gyroscopic matrix is symmetric instead of being skew symmetric.

The 1-D approach does not allow to study the effect of the flexibility of the discs and blades that may play an important role in the dynamics of certain types of rotors, like those of turbines.

The dynamics of blades can be studied by modelling them as radial beams and the dynamics of discs can be studied by using models based on rotating membranes and discs or, in some cases, rotating rings.

However, if the system is not of the simplest type, the theories of rotating beams, membranes, discs and rings do not yield closed form solutions and numerical solutions must be searched. It is thus natural to resort to the FEM also in this case.

An extension of the 1-D models are the so-called 1½-dimensional (1½-D) models, in which shafts are modelled as beams while axi-symmetric elements in which the displacement field is expressed by trigonometric polynomials in the polar angle are used to model the discs and even the rows of blades [4, 5, 6].

When the flexibility of discs and blades is accounted for, a new phenomenon usually referred to as *centrifugal stiffening* appears and the structure of the homogeneous equation (1) becomes [3]

$$\mathbf{M}\ddot{\mathbf{q}} + \Omega\mathbf{G}\dot{\mathbf{q}} + \left(\mathbf{K} + \mathbf{K}_\Omega\Omega^2\right)\mathbf{q} = 0 \tag{2}$$

Centrifugal stiffening is simply explained: discs and blades are stressed by tensile forces in their plane (along their axis for the latter) and this causes an increase of their natural frequency. This effect can be seen as a virtual increase of stiffness, that is proportional to the centrifugal force and thus to the square of the spin speed.

Together with this phenomenon, however, allegedly there is another one that causes a decrease of the natural frequency and is often referred to as *centrifugal softening* [1]. This effect might be strong enough to cause a natural frequency to be equal to zero at a given speed: that speed is often referred to as a critical speed and is a sort of elastic instability. The fact that a natural frequency reduces to zero is not strange in itself: it is exactly what happens in the case of a beam that is subject to compressive axial forces, when the latter are strong enough to cause buckling. What is strange is that a phenomenon of this kind occurs under the effect of a tensile force field, like that due to centrifugal forces.

An instance of this type is reported in [1], on page 286: «the backward whirl natural frequency decrease with speed and the effective stiffness becomes zero when the spin speed becomes the natural frequency of the stationary shaft». A Campbell diagram shows the backward branches dropping to zero.

This, and the whole Campbell diagram of fig. 16.12 in [1] is hardly believable for a number of reasons:

- the speed at which this 'zero' occurs is not so high that this phenomenon has no practical importance,
- no apparent gyroscopic effect is evident, in spite of the fact that the geometry of the rotor is such that gyroscopic effects are predictable and, above all,
- the difference between the Campbell diagram showing these effect and that obtained using the classical 1-D approach (also reported) are such that if the first is correct we should draw the conclusion that all results obtained from classical rotordynamics are, at best, a bad approximation and, at worst, completely wrong.

These results are obtained using a 3-dimensional FEM approach.

It is almost 30 years that 3-dimensional (3-D) FEM rotordynamics is one of the main goals in the field, we can say in a figurate way that it represents *the Holy Grail of rotordynamics*.

This is mainly not because the 1-D and 1½-D approaches are not accurate enough for most rotordynamics studies, but for an eminently practical reason. When a rotating machine is designed using CAD, and a 3-D mesh is automatically generated from the 3-D CAD drawings for performing the static and quasi-static analysis, it would be quite expedient to use the same

model, already available, also for the rotordynamic studies, instead of having to build another 1-D model followed perhaps by a further 1½-D model.

The point is that if the mentioned Campbell diagram is typical of 3-D rotordynamics, serious doubts can be cast on the whole approach.

The aim of the present paper is trying to understand the elusive *centrifugal softening effect*, a sort of a ghost that haunts rotordynamics since decades, and to make the point on the 3-D FEM approach. To achieve this goal some analytical solutions that are available in the literature for the rotating beam and the rotating ring are re-examined with the aim of finding traces of *centrifugal softening* and then FEM rotordynamics is re-examined.

2. Rotating beams

The simplest rotating system for which a softening effect due to rotation is quoted in the literature [1] is the rotating beam. Since for this system an equation of motion can be written analytically and solved numerically without too many difficulties it is worthwhile to study this case with the aim of understanding whether the alleged softening effects actually exists.

2.1 In plane behavior

The study reported in [1] regards the in-plane dynamics of a beam attached at the periphery of a rigid disc rotating at an angular velocity Ω that is not assumed to be constant. The assumption that the angular acceleration α is constant is then introduced, so that

$$\Omega = \Omega_0 + \alpha t \tag{3}$$

Although the inertia of the cross section of the beam and shear deformations are accounted for, and thus the beam should be of the Timoshenko type, in some points some assumptions typical of the Euler-Bernoulli beam are made, but this has little importance in this context. By applying the Hamilton's Principle, after several pages of complex computations, the following dynamic equilibrium equation is obtained

$$\begin{aligned} &\ddot{y} + \tfrac{I_{xx}}{A}\,\ddot{y}'' + \tfrac{EI_{xx}}{\rho A}\,y'''' + (\Omega_0 + \alpha t)^2\left[(R+Z)y' - y - R_2 y''\right] + \\ &\quad + 2(\Omega_0 + \alpha t)\left(\dot{y}y' - y''\int_o^l \dot{y}\,dz - \int_o^l y'\,\dot{y}'\,dz\right) + \\ &\quad + \alpha\left(yy' - \frac{1}{2}\int_o^l y'^2\,dz - y''\int_o^l y\,dz\right) + \alpha(R+Z) = 0 \quad , \end{aligned} \tag{4}$$

where the symbols are those used in [1]. Rewriting it using the symbols reported in fig. 1a, it becomes

$$\ddot{v}+\tfrac{I_z}{A}\ddot{v}''+\tfrac{EI_z}{\rho A}v''''+(\Omega_0+\alpha t)^2\left[rv'-v-\frac{1}{2}\left(r_o^2-r^2\right)v''\right]+$$
$$+2(\Omega_0+\alpha t)\left(\dot{v}v'-v''\int_{r_i}^{r}\dot{v}dr-\int_{r_i}^{r}v'\dot{v}'dr\right)+ \qquad (5)$$
$$+\alpha\left(vv'-\frac{1}{2}\int_{r_i}^{r}v'^2\,dr-v''\int_{r_i}^{r}vdr\right)+\alpha r=0\ .$$

Even if not explicitly stated, the equation refers to a prismatic homogeneous beam (E, A and ρ are constant). The term in $(R+Z)y'$ (i.e. rv') in the first line is labelled as 'Stiffness due to rotation – Hardening' and the terms in y and R_2y'' (i.e. in v and v'') are labelled as 'Stiffness due to rotation – Softening', apparently because the first has a sign (+) and the others a sign (–).

The terms in the second line are labelled as 'nonlinear Coriolis forces', while the terms on the last line are labelled as 'depending on the acceleration'.

If Eq. (5) is linearized to study the bending in-plane vibration of the beam, it follows

$$\ddot{v}+\tfrac{I_z}{A}\ddot{v}''+\tfrac{EI_z}{\rho A}v''''+(\Omega_0+\alpha t)^2\left[rv'-v-\frac{1}{2}\left(r_o^2-r^2\right)v''\right]+\alpha r=0\ . \qquad (6)$$

No shear deformation is accounted for, so that the beam is neither an Euler Bernoulli nor a Timoshenko beam. If shear deformation is neglected, it is better to neglect also rotational inertia (otherwise inconsistent simplifications are made [2]). If the angular velocity is assumed to be constant, the equations reduces to

$$\ddot{v}+\tfrac{EI_z}{\rho A}v''''+\Omega^2\left[rv'-v-\frac{1}{2}\left(r_o^2-r^2\right)v''\right]=0\ . \qquad (7)$$

This equation coincides with Eq. (13.54) (with ψ = 90°) on page 480 in [3], where the equation is obtained directly using Lagrange equations.

Out of the three terms in Ω^2,

R_2y'' (or $\frac{1}{2}(r_o^2-r^2)y''$) is only apparently negative. For instance, if the shape $y(z)$ is harmonic in the space coordinate (like in the case of a vibrating non-rotating beam) the sign of y'' is opposite to the sign of y, and thus this term has the same sign of the first one that is considered positive. Actually, if the genesis of this term is considered, this is the true *stiffening* term that is found in beams and is accounted for by the *geometric* matrix in the FEM.

Term $(R+Z)y'-y$ (or $rv'-v$) is a sort of *rotating pendulum* term due to the fact that the centrifugal force F_c in fig. 1c is directed radially. The

restoring force acting on a length *dr* of the pendulum with cross sectional area *A* and density ρ is thus

$$F_r = F_c \sin(\vartheta - \alpha) \approx \frac{\rho A \Omega^2}{r}(rv' - v)dr \quad . \tag{8}$$

The negative term is thus just a subtractive term to decrease the restoring force due to the fact that it is directed along OP and not along CP. The positive part is anyway always larger than the negative one.

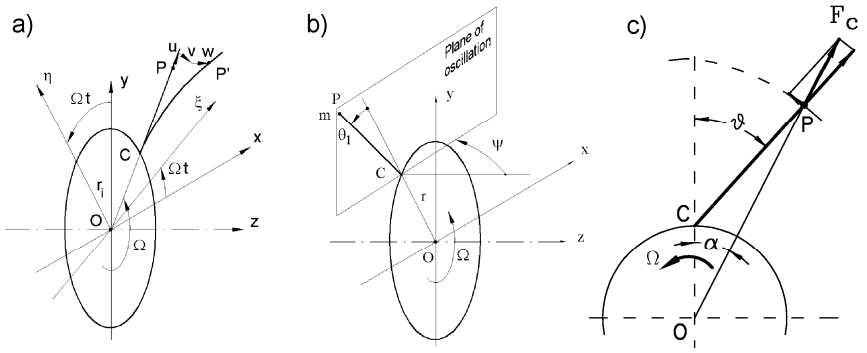

Fig. 1: a): Rotating beam; b) Rotating pendulum oscillating in the rotation plane ($\psi = 90°$); c) Forces acting on a rotating pendulum in the rotation plane.

The rotating pendulum is thus subjected to no *centrifugal softening* effect and its natural frequencies can be expected to increase monotonically with the rotation speed.

As an added consideration, we can see that there is no Coriolis or gyroscopic term, at least within the frame of the linearized theory for the in-plane behaviour of rotating beams.

2.2 Out-of-plane behavior

Consider a rotating beam oscillating in a direction that is perpendicular to the rotation plane.

Its linearized equation of motion is the same Eq. (13.54) on page 480 in [3] but with $\psi = 0$ (i.e. with the axial displacement *w* instead of the in plane displacement *v*) and the moment of inertia of the cross section about a different axis

$$\ddot{w} + \frac{EI_x}{\rho A} w'''' + \Omega^2 \left[rw' - \frac{1}{2}\left(r_o^2 - r^2\right) w'' \right] = 0 \quad . \tag{9}$$

Again there is no centrifugal softening effect and no linear Coriolis or gyroscopic effect.

2.3 Extensional behavior

The above equations were obtained by neglecting the deformation of the beam along its axis. i.e. by assuming that the beam is inextensible. This assumption is well justified, since the axial frequencies of the beam are much higher than those that are usually considered in rotordynamics.

Consider the dynamic equilibrium equations of a rotating string (Eq. (13.31), page 474 in [3], add the restoring forces due to the stiffness of the beam and include the explicit expression of the generalized forces (Eq. (13.32), *ibid*.). The equations of motion are:

$$\begin{cases} \rho A\left[\ddot{u} - \Omega^2\left(r+u\right) - 2\Omega\dot{v}\right] - EA\dfrac{\partial^2 u}{\partial r^2} = \dfrac{\partial T}{\partial r} \\ \rho A\left[\ddot{v} - \Omega^2 v + 2\Omega\dot{u}\right] - EI_y\dfrac{\partial^4 v}{\partial r^4} = \dfrac{\partial}{\partial r}\left(T\dfrac{\partial v}{\partial r}\right) \\ \rho A\ddot{w} - EI_z\dfrac{\partial^4 w}{\partial r^4} = \dfrac{\partial}{\partial r}\left(T\dfrac{\partial w}{\partial r}\right) \end{cases} \tag{10}$$

where T is the axial tensile force acting on the beam.

Assume that displacements are small enough not to affect the axial tensile force in the beam. From the first equation it follows

$$\frac{\partial T}{\partial r} = -\rho A r\Omega^2 \quad . \tag{11}$$

If the lateral displacements are neglected, the first equation can be solved in an uncoupled way, obtaining

$$\rho A\left[\ddot{u} - \Omega^2 u\right] - EA\frac{\partial^2 u}{\partial r^2} = 0 \quad . \tag{12}$$

Operating in the same way as usual in the computation of the axial vibration of beams, the time history of the axial motion can be assumed to be harmonic with frequency ω, yielding

$$u\left(\omega^2 + \Omega^2\right) + \frac{E}{\rho}\frac{\partial^2 u}{\partial r^2} = 0 \quad . \tag{13}$$

The axial natural frequencies of the beam (clamped at the root and free at the other end) at standstill are

$$\omega_{i0} = \frac{i\pi}{(r_o - r_i)}\sqrt{\frac{E}{\rho}} \qquad \text{for } i = 1, 2, \ldots \tag{14}$$

The natural frequencies of the rotating beam are thus

$$\omega_i = \sqrt{\omega_{i0}{}^2 - \Omega^2} \quad . \tag{15}$$

It seems that in this case a centrifugal softening effect exists, after all.

When the speed equals the natural frequency at standstill, the natural frequency reduces to zero, meaning that a sort of elastic instability is reached. However, such a speed can never be reached, because the centrifugal stresses exceed by at least one or two orders of magnitude the allowable strength of any material.

Moreover, it is the whole centrifugal softening effect that is in practice so small that it can be considered negligible.

Consider a beam with a radii ratio $\chi = r_i/r_o$. The maximum stress at the root is

$$\sigma = \frac{\rho\Omega^2 r_o^2}{2}(1-\chi^2) \quad . \tag{16}$$

The relationship linking the speed and the stress is thus

$$\Omega^2 = \frac{2\sigma}{\rho r_o^2 (1-\chi^2)} \quad . \tag{17}$$

The natural frequencies of the rotating beam are thus

$$\omega_i = \omega_{i0}\sqrt{1 - \frac{2(1-\chi)}{i^2\pi^2(1+\chi)}\frac{\sigma}{E}} = \frac{i\pi}{(r_o - r_i)^2}\sqrt{\frac{E}{\rho}}\sqrt{1 - \frac{2(1-\chi)}{i^2\pi^2(1+\chi)}\frac{\sigma}{E}} \quad . \tag{18}$$

The *correction factor* due to rotation is limited by the ratio σ/E allowable for the material and depends also on geometry, i.e. on ratio χ.

The reduction of the first axial natural frequency of a prismatic homogeneous beam is reported in fig. 2 as a function of the maximum axial strain $\varepsilon = \sigma/E$ for different values of χ. An approximate value of the axial strain that causes failure of different materials is also reported.

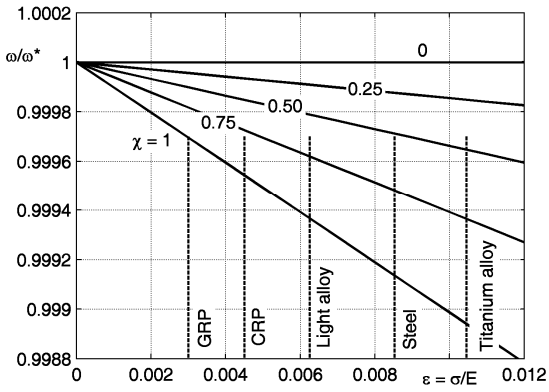

Fig. 2: Reduction of the first axial natural frequency of a prismatic homogeneous beam as a function of the maximum axial strain $\varepsilon = \sigma/E$ for different values of χ. Approximate values of the maximum strain at failure for AISI 4340 steel, 2024 light alloy, ZK60 titanium alloy, GRP and high modulus CRP are also reported.

From the figure, it is clear that the maximum decrease of the natural frequency due to rotation is smaller than 0.1%.

As a conclusion, it is possible to state that no softening effect due to centrifugal stressing is present on rotating beams, except for a very small reduction (much less than 1%) of some very high frequency extensional modes that are almost never considered, and even this only at speeds close to failure speeds of the rotor.

Also no gyroscopic or Coriolis effect have been found, except when there is an interaction between extensional (usually neglected) and bending modes.

3. Rotating rings and circular shells

The problem of finding the natural frequencies and mode shapes of a ring, either non-rotating [7] or rotating [3, 8-11] is a classical one and has been tackled a good number of times, by different authors with different sets of assumptions, obtaining different solutions. These solutions were also extended to cylindrical shells.

In general it must be said that these solutions, many of which had also been validated through physical or numerical experiments, are quite close to each other to the point that it has been stated that *from the physical point of view, one cannot judge which theoretical model is better* [9, 11].

The most common solutions are *inextensional*, i.e. solutions in which the stiffness of the ring along its circumference is assumed to be infinitely high.

3.1 Inextensional solution

Out-of-plane vibration

Owing to symmetry reasons, in-plane vibration (i.e. vibration in *xy* plane of fig. 3) uncouples from out-of-plane vibration.

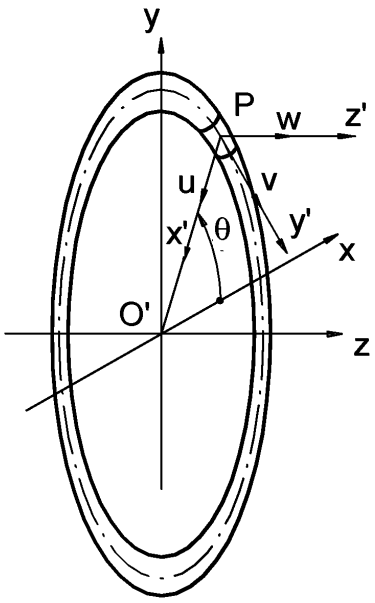

Fig. 3: Sketch of a ring rotating about the *z*-axis.

The simplest solution deals with a thin ring, i.e. a ring thin enough to neglect shear deformation in bending and the contribution to the kinetic energy due to the rotation of the cross section about its axis (*z'* axis for in-plane and *x'* axis for out-of-plane deformations). The ring is thus the equivalent of an Euler-Bernoulli beam, except for the fact that it is not straight.

The solution reported in [3] for the out-of-plane vibration is

$$\omega_i = \sqrt{\frac{EI_x}{\rho A r^4}\frac{\kappa i^2\left(1-i^2\right)^2}{\left(1+\kappa i^2\right)}+i^2\Omega^2} = \sqrt{\omega_{i0}^2+i^2\Omega^2} \quad . \qquad (19)$$

where

$$\kappa = \frac{GI'_p}{EI_x} \quad .$$

is the shear factor that, in case of circular or annular cross section, is equal to $1/(1 + \nu)$.

The out-of-plane natural frequencies thus always increase with the speed.

The frequencies so computed are referred to a reference frame that rotates together with the ring. Each mode produces two travelling waves, one moving forward in the fixed (inertial) frame and one moving backward. The resulting frequencies are:

- Forward travelling wave:

$$\omega_{Fi} = i\Omega + \sqrt{\frac{EI_x}{\rho A r^4}\frac{\kappa i^2\left(1-i^2\right)^2}{\left(1+\kappa i^2\right)} + i^2\Omega^2} = i\Omega + \sqrt{\omega_{i0}^2 + i^2\Omega^2} \quad . \tag{20}$$

- Backward travelling wave:

$$\omega_{Bi} = i\Omega - \sqrt{\frac{EI_x}{\rho A r^4}\frac{\kappa i^2\left(1-i^2\right)^2}{\left(1+\kappa i^2\right)} + i^2\Omega^2} = i\Omega - \sqrt{\omega_{i0}^2 + i^2\Omega^2} \quad . \tag{21}$$

The nondimensional frequencies in the rotating and fixed frame are reported in fig. 4 as functions of the nondimensional speed. The backward modes are always backward in the whole speed range (Eq. (21) yields always a negative result) and the Campbell diagram is very similar to that of a simple 4-degrees of freedom rotor [3] and shows the presence of a Coriolis or gyroscopic effect of the usual type.

It must be noted that the frequency of the mode with $i = 0$, corresponding to a translation of the ring in axial (z) direction, and the mode with $i = 1$ corresponding to a rotation of the ring on/around the x or the y axes are equal to 0. As expected they are rigid body modes since the ring is free; the other modes are deformation modes.

It must also be noted that the modes with $i > 1$ are of little relevance in rotordynamic studies, since they cannot couple with the bending motions of the rotor as a whole [4, 5]. They are a sort of local modes of the ring.

All forward modes lie above the $\omega = \Omega$ line, and thus are in the supercritical regime, as expected from a high frequency deformation mode.

As a conclusion, also here no centrifugal softening effect can be found, while a gyroscopic effect is present when the natural frequencies are considered in a fixed reference frame.

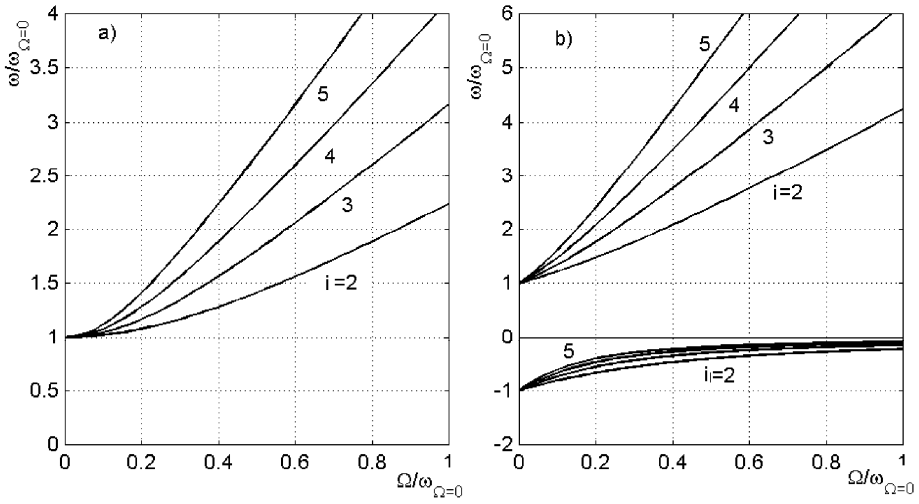

Fig. 4: Nondimensional natural frequencies as functions of the nondimensional spin speed for the out-of-plane vibrations of a rotating ring; mode shapes with i = 2, 3, 4 and 5. (a) Frequencies in the rotating frame; (b) forward and backward frequencies in the inertial frame.

In-plane vibration

The classical solution for the inextensional in-plane vibration of a thin non-rotating ring ring dates back to the 19th century [12, 13]. Rotation was later added, obtaining [14, 3]

$$\omega_i = \frac{i}{i^2+1}\left[-2\Omega \pm \left(i^2-1\right)\sqrt{\left(1+i^2\right)\frac{EI_z}{\rho A r^4}+\Omega^2}\right] \quad . \tag{22}$$

This solution, referred to the rotating frame, yields two standing waves: one in forward direction (the smaller one in absolute value, solution with sign '+'), and one in backward direction (the larger one, solution with sign '-').

Writing the solution in the inertial frame, it follows

$$\omega_i = \frac{i\left(i^2-1\right)}{i^2+1}\left[\Omega \pm \sqrt{\left(1+i^2\right)\frac{EI_z}{\rho A r^4}+\Omega^2}\right] \quad . \tag{23}$$

These results are reported in fig. 5. Also in this case there is no centrifugal softening effect, except for a small decrease of the lowest forward frequency computed in the rotating frame. However, from Eq. (23) and fig. 5b, it is clear that more than centrifugal softening effect this is a Coriolis effect.

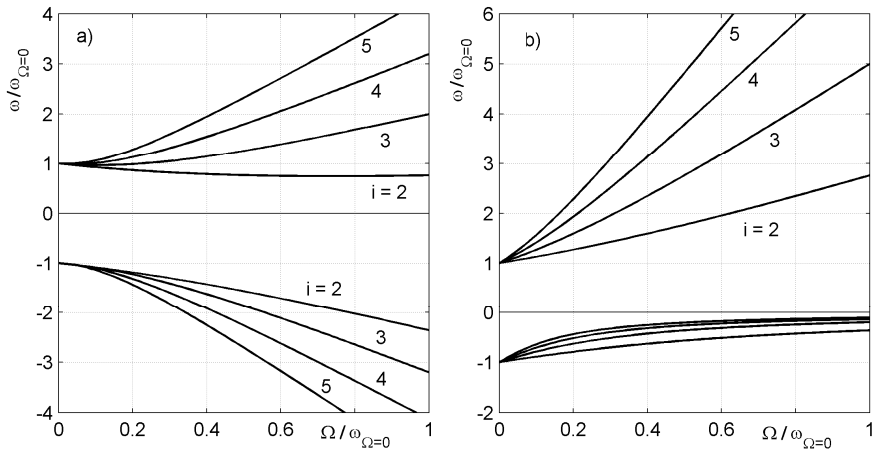

Fig. 5: Nondimensional natural frequencies as functions of the nondimensional spin speed for the in-plane vibrations of a rotating ring; mode shapes with $i = 2, 3, 4$ and 5. (a) Frequencies in the rotating frame; (b) forward and backward frequencies in the fixed frame.

3.2 Extensional solution

The inextensional solution yields no centrifugal softening effect, but this does not mean that this effect does not exist. In [14] it is clearly stated that *strong coupling exists between the extensional type deformation and bending type deformation*, and that this coupling is particularly important in thick rings. The many assumptions made above may hide a softeng effect that after all is present.

The analytical solution for the extensional thick ring is quite complex.

A solution for the in-plane extensional natural frequency can be found in [9]. From Eq. (5) in [9] the characteristic equation can be derived in the form

$$\det\begin{bmatrix} \left(i^2-1\right)^2+\alpha-\omega^{*2}+i^2\Omega^{*2} & j\left[\alpha i-2\Omega^*\left(\omega^*-i\Omega^*\right)\right] \\ -j\left[\alpha i-2\Omega^*\left(\omega^*-i\Omega^*\right)\right] & \alpha i^2-\omega^{*2}+i^2\Omega^{*2} \end{bmatrix}=0 \quad , \tag{24}$$

where j is the imaginary unit, the nondimensional frequency and speed are

$$\omega^* = \omega\sqrt{\frac{\rho A r^4}{EI_z}} \quad \text{and} \quad \Omega^* = \Omega\sqrt{\frac{\rho A r^4}{EI_z}}$$

and the nondimensional parameter

$$\alpha = \frac{Ar^2}{I_z} = \left(\frac{r}{r_g}\right)^2$$

where r_g is the radius of inertia of the cross section of the ring, is a parameter that states the importance of extensional deformation.

The value of α is usually quite high; for instance, if the ring has a rectangular cross section with a radial thickness equal to $1/10^{th}$ of the radius, $\alpha = 1200$.

If r_g is small (α is large) the inextensional theory is accurate, while if its value is low the ring is thick and extensional deformations must be accounted for. Note that when α is low, at any rate the assumptions on which the solution is based break down (the ring is no more an Euler-Bernoulli beam).

Each mode has now two pairs of solutions instead of one: the first (lowest) pair is linked with bending vibration and tends to that of the inestensional solution when α tends to infinity; the other one is much higher and is related with the mainly extensional vibration. The first pair has a zero value for $i = 1$, since in this case the first mode is a rigid-body mode.

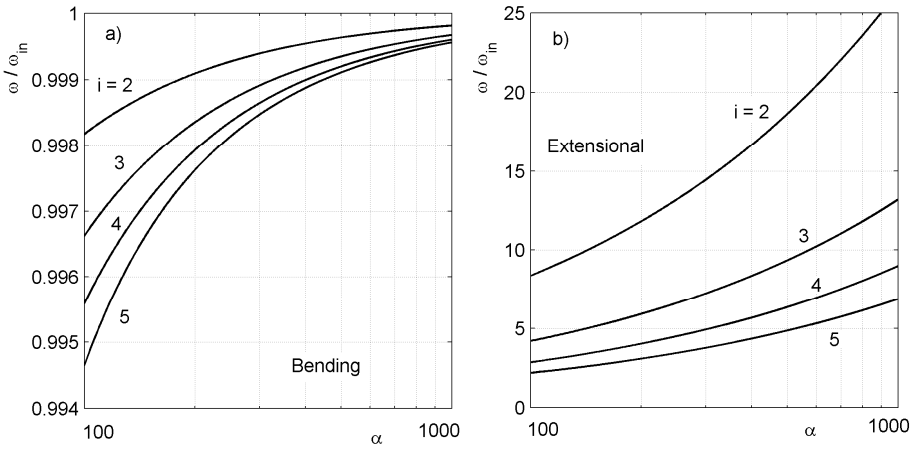

Fig. 6: Effect of extensional deformation on the in-plane frequencies of non-rotating ring. Ratio between the solution computed taking into account extensional deformations and the inextensional solution as a function of parameter α (note that a value $\alpha = 100$ is too low to allow the thin ring theory to hold).

The effect of the extensional deformation on the in-plane vibration of the nonrotating ring can be seen in figure 6, where the ratio between the

extensional and the inextensional solution is plotted as a function of α for i = 2, …, 5.

The solution for α = 1000 is reported in fig. 7. The frequencies in the fixed frame of the mainly bending modes are plotted in fig. 7a, together with the inextensional solution. The difference between the two solutions is quite small. The frequencies, always in the fixed frame, of the mainly extensional modes are plotted in fig. 7b.

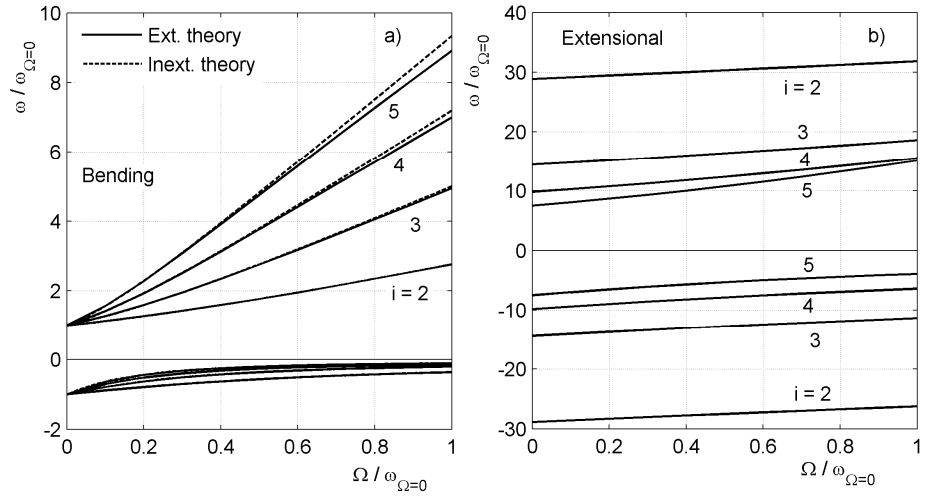

Fig. 7: Nondimensional natural frequencies (referred to the fixed frame) as functions of the nondimensional spin speed for the in-plane vibrations of a rotating ring; mode shapes with i = 2, 3, 4 and 5. (a) Mainly bending modes, results of the extensional theory compared with those of the inextensional theory; (b) Mainly extensional modes.

The conclusions that can be drawn from fig. 7 are the same obtained from the inextensional theory: no centrifugal softening was found, while a certain Coriolis or Gyroscopic effect is clear.

However, this does not mean that a centrifugal softening effect cannot be found in any circumstance. To repeat what was done in the case of the rotating beam, consider the mode with $i = 0$, a rigid body mode when only bending is considered. From the extensional theory the frequency of this mode can be found from the characteristic equation:

$$\omega^{*2}\left(\omega^{*2} - \alpha - 1 - 4\Omega^{*2}\right) = 0 \tag{25}$$

A solution is $\omega = 0$, corresponding to the rigid body inextensional mode, while another solution is

$$\omega^* = \pm\sqrt{\alpha + 1 + 4\Omega^{*2}} \quad , \tag{26}$$

corresponding to the extensional modes. This solution yields a natural frequency that, unlike what was seen in the case of rotating beams, is always growing with the speed. In this case no centrifugal softening effect exists, even at rotational speeds which no material can withstand.

4. FEM modelling: 1½ dimensional approach

The common 'beam' approach to FEM modelling of rotors cannot take into account either centrifugal stiffening or softening, since shafts are modelled as beams and discs as rigid bodies.

The simplest approach in which these effects can be accounted for is the so-called 1½ dimensional approach, consisting in modelling shafts as beams and using axi-symmetric elements in which the displacement field is expressed by trigonometric polynomials in the polar angle for discs [4 -6].

The linearized homegenous equation of motion for the free vibration of an undamped, axy-symmetrical rotor modelled using such elements is (Eq. (43) in [4])

$$\begin{cases} \mathbf{M}_{ax}\ddot{\mathbf{q}}_{ax} + \left(\mathbf{K}_{ax} + \Omega^2\mathbf{K}_{\Omega ax}\right)\mathbf{q}_{ax} = 0 \\ \mathbf{M}_{tor}\ddot{\mathbf{q}}_{tor} + \left(\mathbf{K}_{tor} + \Omega^2\mathbf{K}_{\Omega tor}\right)\mathbf{q}_{tor} = 0 \\ \mathbf{M}_{inp}\ddot{\mathbf{q}}_{inp} - j\Omega\mathbf{G}_{inp}\dot{\mathbf{q}}_{inp} + \left(\mathbf{K}_{inp} + \Omega^2\mathbf{K}_{\Omega inp} - \Omega^2\,\mathrm{M}_{ninp}\right)\mathbf{q}_{inp} = 0 \\ \mathbf{M}_{out}\ddot{\mathbf{q}}_{out} - j\Omega\mathbf{G}_{out}\dot{\mathbf{q}}_{out} + \left(\mathbf{K}_{out} + \Omega^2\mathbf{K}_{\Omega out} - \Omega^2\,\mathrm{M}_{nout}\right)\mathbf{q}_{out} = 0 \end{cases} \tag{27}$$

The first equation, characterized by the subscript '*ax*' deals with the axial behaviour, the second one, characterized by the subscript '*tor*' deals with the torsional behaviour, the third equation, characterized by the subscript '*inp*' deals with the in-plane bending behaviour, the last equation, characterized by the subscript '*out*' deals with the out-of-plane bending behaviour. The four equations are uncoupled, owing to the 'beamlike' assumptions typical of the 1½ dimensional approach and to the axial symmetry of the rotor.

The last two equations are written using the complex-coordinates approach, leading to complete symmetry of all relevant matrices, including the gyroscopic matrices. The complex-coordinates approach is applicable also in the case the stator or even the rotor are not axially symmetrical, but in such cases the equations of motions are different from Eq. (27). In the latter case the equations written in the inertial frame are non-time-invariant [15].

The equations of motion can be assembled together yielding

$$\mathbf{M}\ddot{\mathbf{q}} + \Omega\mathbf{G}\dot{\mathbf{q}} + \left(\mathbf{K} + \Omega^2\mathbf{K}_\Omega - \Omega^2\,\mathrm{M}_n\right)\mathbf{q} = 0 \quad . \tag{28}$$

In this formulation the uncoupling is no more required and the complex-coordinates is not used: the gyroscopic matrix is thus skew-symmetric while all other matrices are symmetric.

Equation (28) can be considered as a general equation for FEM rotordynamics, and can be derived also in the case of bladed discs [5].

- Matrix **G** is a gyroscopic matrix, so the gyroscopic effect is present (and plays an important part) in FEM rotordynamics.
- Matrix $\mathbf{K}_\Omega$ is the centrifugal stiffening matrix. It is what is usually called a geometric matrix and in this case is proportional to the square of the spin speed. Other geometric effects, like those due to temperature gradients in turbine rotors, may be present but, since they are not linked to the spin speed, are implicitly included in matrix **K**.
- Matrix $\mathbf{M}_n$ is the centrifugal softening matrix, which is definitely included in all FEM rotordynamics equations. It usually causes a decrease of the natural frequencies with the speed (at least if it is positive defined). To assess whether the natural frequencies actually decrease or not with increasing speed, it must be assessed whether the effect of $\mathbf{M}_n$ is stronger than the effect $\mathbf{K}_\Omega$ or not.

By assuming a solution of the type

$$\ddot{\mathbf{q}} = \mathbf{q}_0 e^{j\omega t} \tag{29}$$

the following frequency domain characteristic equation is obtained

$$\det\left(-\omega^2\mathbf{M} + j\omega\Omega\mathbf{G} + \mathbf{K} + \Omega^2\mathbf{K}_\Omega - \Omega^2\mathbf{M}_n\right) = 0 \tag{30}$$

In [1, 16] the following frequency domain equation is reported (Eq. (16.31) in [1])

$$\det\left(-\omega^2\mathbf{M} + \mathbf{K} - \Omega^2\mathbf{M}\right) = 0 \tag{31}$$

It must be noted that in fig. 16.12 in [1] the frequencies for the forward branch and the backward branch of each mode are different, which is not justified by Eq. (31) that has solutions with identical absolute values and opposite sign.

The differences between Eq. (31) and Eq. (30) are three, namely in Eq. (31)

- the gyroscopic matrix **G** is missing,
- the centrifugal stiffening matrix $\mathbf{K}_\Omega$ is missing,
- matrix **M** is substituted for matrix $\mathbf{M}_n$.

The first 2 points may be of little importance if the rotor is radially thin (but at this point one wonders why using the FEM at all for a structure that is necessarily beamlike).

The actual point is the third one, and concerns the structure of matrix $\mathbf{M}_n$.

In [4] the structure of matrices $\mathbf{M}$ and $\mathbf{M}_n$ for both in-plane and out-of-plane motions is shown to be (Eq. (44) in [4]):

$$\mathbf{M}_{inp} = \begin{bmatrix} m & \mathbf{m}_{inp1} & \mathbf{m}_{inp1} \\ \mathbf{m}_{inp1}^T & \mathbf{m}_{inp2} & \mathbf{0} \\ \mathbf{m}_{inp1}^T & \mathbf{0} & \mathbf{m}_{inp2} \end{bmatrix}, \quad \mathbf{M}_{ninp} = \begin{bmatrix} 0 & \mathbf{0} & \mathbf{0} \\ \mathbf{0} & \mathbf{m}_{inp2} & -\mathbf{m}_{inp2} \\ \mathbf{0} & -\mathbf{m}_{inp2}^T & \mathbf{m}_{inp2} \end{bmatrix}, \quad (32)$$

$$\mathbf{M}_{out} = \begin{bmatrix} J_t & -\mathbf{m}_{out1} \\ -\mathbf{m}_{out1}^T & \mathbf{m}_{out2} \end{bmatrix}, \quad \mathbf{M}_{nout} = \begin{bmatrix} 0 & \mathbf{0} \\ \mathbf{0} & \mathbf{m}_{out2} \end{bmatrix}$$

The matrices are partitioned in the way described in [4] but the details of this and the meaning of the symbols indicating the various submatrices are not relevant here. What matters is that the mass matrices and the centrifugal softening matrices are different and that some of the lines and columns of the latter are equal to zero. This means that not all degrees of freedom participate to the centrifugal softening effect. This is exactly the same thing that was found for the cases of the rotating beam and ring.

Equation (31) is thus incorrect.

5. FEM modelling: 3-dimensional approach

The application of three-dimensional FEM modelling to rotordynamics is not straightforward. Probably the first paper on the subject [17] dates back to 1984; since then a certain number of papers on the subject were published, but perhaps not so many as could be expected due to the importance of the subject.

In rotordynamics the issues of whether the rotor is axially symmetrical and the definition of the exact kinematics of the deformation are of paramount importance.

In case of 1-D or 1½-D FEM models the axial symmetry of the rotor (or its lack of axial symmetry, if some of the beams have a cross section that is not such) is immediately assessed from the properties of the elements used. In a 3-D model axial symmetry it is not a property of the elements, but of the mesh and, as such, it cannot be easily assessed. Moreover, it is well known that between the case of no axial symmetry and true axial symmetry there is the case of cyclic symmetry. If cyclic symmetry has an order equal to, or larger than, 3 the global effect is that of axial symmetry (i.e. of cyclic symmetry with order infinity), while the local deformations are not such. In

this case it may be expedient to pass from physical to modal coordinates, so that full axial symmetry is reached [18].

No general purpose FEM code states whether the model is axially symmetrical, and thus the solution does not take different paths following this characteristics, while in rotordynamics this feature is essential.

The details of the reference frames and the kinematics of the element and the structure are described in [19]. By writing as usual the kinetic and potential energy of the element, the homogeneous equations of motion can be obtained through the Lagrange equations

$$\mathbf{M}\ddot{\mathbf{q}} + \Omega\mathbf{G}\dot{\mathbf{q}} + \left(\mathbf{K} + \mathbf{K}_{g\sigma} + \mathbf{K}_{g\varepsilon} + \Omega^2\mathbf{M}_{ni}\right)\mathbf{q} = \mathbf{0} \quad , \tag{33}$$

where $\mathbf{G}$ is the gyroscopic matrix, typical of rotordynamic problems, $\mathbf{K}_{g\sigma}$ and $\mathbf{K}_{g\varepsilon}$ are the pre-stress and pre-strain stiffness matrices and $\mathbf{M}_{ni}$ (or $\mathbf{K}_{ni}$) is a matrix linked to the fact that the frame to which the eqution is referred to in non-inertial. The last 3 matrices come from the general approach adopted in [19].

Since matrix $\mathbf{K}_{g\sigma}$ may contain a part that is proportional to Ω^2, the structure of Eq. (33) is identical to that of Eq. (28).

An example of a simple FEM solution for a 3_D rotordynamic model is shown in fig. 8a. The example deals with a ring, with inner radius of 490 mm, outer radius of 510 mm and axial width of 50 mm, built using a light alloy with a Young Modulus $E = 7.31 \times 10^{10}$ Pa, a density $\rho = 2770$ kg/m^3 and a Poisson Ratio $\upsilon = 0.33$. The ring is modeled using 80 isoparametric 20-nodes brick elements of the type described in [19]. The value of parameter α defined in Eq. (24) is 7,500.

The results in terms of the lowest natural frequencies in the rotor-fixed frame as functions of the spin speed are reported in fig. 8b.

The frequencies of the rigid-body and first in-plane modes computed using the FEM are practically identical to those obtained from the analytical inextensional solution (the lines are completely superimposed). The higher frequencies are increasingly different with increasing order.

The solution obtained from Eq. (31), by using the same stiffness and mass matrices as for the FEM computation, is also shown: it is completely different both from the FEM and the analytical solution.

No centrifugal softening was found in the speed range considered, which is well beyond the possible speed range: at 1000 rad/s the centrifugal stressing in the rim is 692.5 MPa, higher than the allowable strength of light alloys.

The analysis was then repeated reaching higher, completely unrealistic, speeds. The results are reported in fig. 9, in which also the results obtained using the extensional solution are plotted.

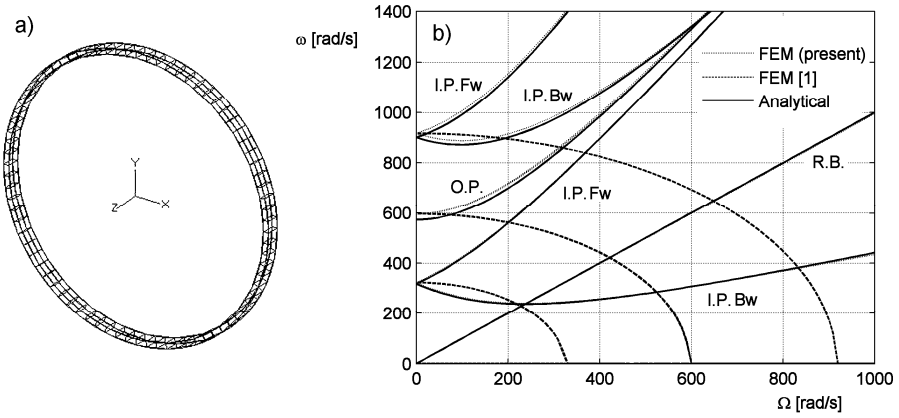

Fig. 8: a): Ring meshed using 80 20-nodes isoparametric elements. b) Campbell diagram including rigid-body (R.B), in-plane backward (I.P. Bw), in-plane forward (I.P. Fw) and out-of-plane (O.P.) modes. The numerical solution obtained using 3-D FEM is compared with the analytical solution and the solution obtained from Eq. (31), by using the same stiffness and mass matrices as for the FEM computation.

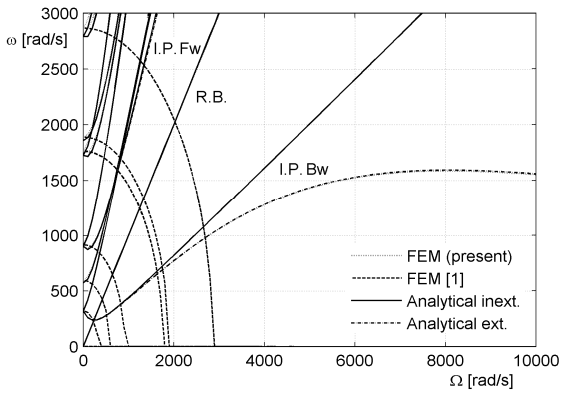

Fig. 9: Same as fig. 8b), but with an extended speed range. Also the analytical extensional solution is reported.

From the fig. 8 it is clear that:

- The analytical extensional solution diverges gradually from the inextensional one starting from 1000 rad/s.
- The present FEM solution is in very close agreement, at least for the first modes, with the analytical solution. Where the extensional solution differs from the inextensional one, the FEM solution follows the former.

Even at very high speed the agreement between the FEM and the analytical solution remains very good.

- At very high speed some centrifugal softening is present. However, a true centrifugal softening of the first backward mode with $i = 2$ (a decrease of the frequency at increasing speed) is found only starting from a speed of about 8,000 rad/s – a speed at which the hoop stress in the ring is above 44,000 MPa!
- The frequencies computed through Eq. (31) have a dependency on the speed that is completely different from that obtained from both the analytical solution and the present FEM model.

Conclusions

Three-dimensional FEM rotordynamics constitutes an important improvement over standard 1-D or 1 ½-D FEM modelling of rotors more from the viewpoint of integrating rotordynamics computations within the standard modelling and analysis practices known as CAE (computer aided engineering), since it allows to use the standard 3-D models generated by CAD and automatically meshed, than from the viewpoint of the accuracy of the results.

However, the 3-D approach introduces some difficulties because it cannot easily distinguish between an axy-symmetric rotor from a non-axysymmetric one. The class of symmetry of the rotor and of the non-rotating parts of the machine must be assessed before starting the analysis, so that it is possible to chose the correct reference frame.

The equation of motion of the rotor is at any rate the same as that common in 1 ½-D analysis, since it contains the usual mass and stiffness matrix common in structural dynamics, plus a skew-symmetric gyroscopic matrix (multiplied by the spin speed) and a symmetric centrifugal stiffening matrix that results from $\mathbf{K}_\Omega - \mathbf{M}_n$ (multiplied by the square of the spin speed). The latter is not the mass matrix changed of sign as stated in Eq. (31).

The effect of the latter matrix is dual: a stiffening effect due to the tensile stresses caused by rotation, and a softening due to the effects of the non-inertial frame in which the equations are written. They combine to give a stiffness net effect, at least unless the speed is very high: both forward and backward branches of the Campbell diagram increase, in absolute value.

The gyroscopic terms have the usual effect seen in elementary rotordynamics: increasing the frequency of forward modes and decreasing (in absolute value) that of backward modes.

In some cases a centrifugal softening effect, i.e. a decrease of the absolute value of the natural frequency of some modes with increasing speed, is found, but it is limited in magnitude and occurs only at speeds so high that cannot be reached without jeopardizing the mechanical integrity of the rotor.

These considerations are obtained from linearized models, but the very concepts of natural frequencies, critical speeds and Campbell diagram can be used only within the range of the values of the various parameters where the system behaves linearly.

The solutions found in the literature where strong softening effects are present must thus be looked at critically.

References

[1] J.S. Rao, *History of Rotating Machinery Dynamics*, Springer, New York, 2011.

[2] G. Genta, *Vibration Dynamics and Control*, Springer, New York, 2009.

[3] G. Genta, *Dynamics of Rotating Systems*, Springer, New York, 2005.

[4] G. Genta and A. Tonoli, *A Harmonic Finite Element for the Analysis of Flexural, Torsional and Axial Rotordynamic Behaviour of Discs*, Journal of Sound and Vibration, 196, 1, 1996, 19-43.

[5] G. Genta and A. Tonoli, *A Harmonic Finite Element for the Analysis of Flexural, Torsional and Axial Rotordynamic Behaviour of Bladed Arrays*, Journal of Sound and Vibration, 207, 5, 1997, 693-720.

[6] G. Genta, C. Feng and A. Tonoli, *Dynamics behavior of rotating bladed discs: A finite element formulation for the study of second and higher order harmonics*, Journal of Sound and Vibration, 239, 25, 2010, 5289-5306.

[7] A.E.H. Love, *A Treatise on the Mathematical Theory of Elasticity*, Dover, New York, 1944.

[8] A. Zohar and J. Aboudi, *The free vibration of a thin circular finite rotating cylinder*, International Journal of Mechanical Science, 15, 1973, 269-278.

[9] M. Endo, K. Hatmura, M. Sakata and O. Taniguchi, *Flexural vibration of a thin rotating ring,* Journal of Sound and Vibration, 92, 2, 1984, 261-272.

[10] W.B. Bickford and E.S. Reddy, *On the in-plane vibration of rotating ring*, Journal of Sound and Vibration, 101, 1, 1985, 13-22.

[11] Y. Chen, H.B. Zhao, Z.P. Shen, I. Grieger and B.H. Kröplin, *Vibrations of High Speed Rotating Shells with Calculations for Cylindrical Shells*, Journal of Sound and Vibration, 160, 1, 1993, 137-160.

[12] R. Hoppe, *The Bending Vibration of a Circular Ring*, Crelle Journal of Mathematics, 73, 1871, 158-170.

[13] G.H. Bryan, *On the Beats in the Vibrations of a Revolving Cylinder of Shell*, Proceedings of the Cambridge Philosophical Society, 7, 1890, 101-111.

[14] J.L. Lin and W. Soedel, *On General in-plane Vibrations of Rotating Thick and Thin Rings*, Journal of Sound and Vibration, 122, 3, 1988, 547-570.

[15] G. Genta, *Whirling of Unsymmetrical Rotors, a Finite Element Approach Based on Complex Coordinates*, Journal of Sound and Vibration, 124, 1, 1988, 27-53.

[16] J.S. Rao, *Rotor Dynamics Comes of Age*, Keynote address, in Proceedings Sixth IFToMM International Conference Rotor Dynamics, Sydney, September 30 – October 3rd, vol. I, 2002, 15.

[17] M. Gerardin and N. Kill, *A new approach to finite element modelling of flexible rotors*, Engineering Computations, 1, 1984, 52-64.

[18] G. Genta and M. Silvagni, *Some Considerations on Cyclic Symmetry in Rotordynamics*, ISCORMA-3, Cleveland, September 2005.

[19] M. Silvagni, G. Genta and A. Tonoli, *Non-Axisymmetrical 3D Element for FEM Rotordynamics*, ISCORMA-2, Gdańsk, Poland, August 4-8 2003.

Symbols

i	order of the mode
j	imaginary unit
$\mathbf{q}$	vector of the generalized coordinates
r	radius
u,v,w	components of the displacement
A	Area of the cross section
E	Joung's modulus
G	shear modulus
$\mathbf{G}$	gyroscopic matrix
I	area moment of inertia
$\mathbf{K}$	stiffness matrix
$\mathbf{K}_\Omega$	speed-dependent stiffness matrix
$\mathbf{M}$	mass matrix
T	kinetic energy, tensile force
U	potential energy
κ	shear factor
σ	stress
ρ	density
υ	Poisson's ratio
χ	radii ratio
ω	frequency
Ω	angular velocity
$\dot{v}$	derivative of v with respect to time
v'	derivative of v with respect to a space coordinate